Article

Solvolysis and Mild Hydrogenolysis of Lignin Pyrolysis Bio-Oils for Bunker Fuel Blends

Antigoni G. Margellou [1,*](ID), Fanny Langschwager [2], Christina P. Pappa [1], Ana C. C. Araujo [3], Axel Funke [3](ID) and Konstantinos S. Triantafyllidis [1,4,5,*](ID)

[1] Department of Chemistry, Aristotle University of Thessaloniki, 54124 Thessaloniki, Greece; x.pappa@yahoo.gr
[2] Department of Piston Machines and Internal Combustion Engines, University of Rostock, 18059 Rostock, Germany; fanny.langschwager@uni-rostock.de
[3] Institute of Catalysis Research and Technology (IKFT), Karlsruhe Institute of Technology (KIT), Hermann-von-Helmholtz Platz 1, 76344 Eggenstein-Leopoldshafen, Germany; ana.araujo@kit.edu (A.C.C.A.); axel.funke@kit.edu (A.F.)
[4] Chemistry Department, King Fahd University of Petroleum and Minerals, Dhahran 31261, Saudi Arabia
[5] Interdisciplinary Research Center for Refining and Advanced Chemicals, King Fahd University of Petroleum & Minerals, Dhahran 31261, Saudi Arabia
[*] Correspondence: amargel@chem.auth.gr (A.G.M.); ktrianta@chem.auth.gr or k.triantafyllidis@kfupm.edu.sa (K.S.T.)

Abstract

The projected depletion of fossil resources has initiated research on new and sustainable fuels which can be utilized in combination with conventional fuels. Lignocellulosic biomass, and more specifically lignin, can be depolymerized towards phenolic and aromatic bio-oils which can be converted downstream into bunker fuel blending components. Within this study, solvolysis under critical ethanol conditions and mild catalytic hydrotreatment were applied to heavy fractions of lignin pyrolysis bio-oils with the aim of recovering bio-oils with improved properties, such as a lower viscosity, that would allow their use as bunker fuel blending components. The mild reaction conditions, i.e., low temperature (250 °C), short reaction time (1 h) and low hydrogen pressure (30–50 bar), led to up 65 wt.% recovery of upgraded bio-oil, which exhibited a high carbon content (63–73 wt.%), similar to that of the parent bio-oil (68.9 wt.%), but a lower oxygen content and viscosity, which decreased from ~298,000 cP in the parent lignin pyrolysis oil to 526 cP in the hydrotreated oil, with a 10%Ni/Beta catalyst in methanol, and which was also sulfur-free. These properties permit the potential utilization of the oils as blending components in conventional bunker fuels.

Keywords: lignin pyrolysis bio-oils; hydrogenolysis; bunker fuel blends; bifunctional catalysts

1. Introduction

During the last several decades, lignocellulosic biomass derived via agricultural and relevant food industry wastes has been recognized as a promising feedstock with which to produce chemicals and renewable fuels. Cellulose, hemicellulose and lignin are the main components of lignocellulosic biomass and can be converted into bio-/renewable jet fuels via thermocatalytic processes [1–3]. Lignin is an amorphous phenolic biopolymer which is mainly derived as a by-product of the pulp and paper industry. More recently, integrated biorefinery processes have been developed, based on organosolv, hydrothermal, alkaline and other biomass pretreatment/fractionation methods, that aim at the selective isolation of both lignin and carbohydrate pulp [4–7]. The isolated lignin exbibits high potential exploitation options. Lignin can be directly utilized in the production of resins, substituting

petroleum-derived phenolic compounds; in asphalt pavements, as a substitute for bitumen; and even in pharmaceutical and biomedical applications, due to its good antioxidant properties [8–14]. Otherwise, lignin can be depolymerized towards bio-oils enriched in phenolic and aromatic compounds. The depolymerization of lignin can be performed via fast pyrolysis, catalytic hydrogenolysis or hydrothermal liquefaction, while a "lignin-first" approach is also used for the simultaneous isolation of lignin monomer/oligomer phenolic compounds and hemicellulose sugars directly from lignocellulosic biomass [15–20]. Fast pyrolysis and hydrogenolysis are the two most common processes which are applied at pilot scale for the production of lignin bio-oils. Fast pyrolysis is performed at 400–600 °C under an inert atmosphere for the production of bio-oil (30 wt.%), gases and char [21–23]. The yield and the composition of bio-oils is strongly dependent on the reaction conditions and the composition of the lignin used as a feedstock. Furthermore, the addition of a catalyst during pyrolysis may induce several reactions (dealkoxylation, dehydration, etc.), resulting in bio-oils enriched in alkylated phenols and aromatics [21–23]. On the other hand, lignin hydrogenolysis is carried out under reductive conditions using hydrogen gas or hydrogen donor solvents (alcohols, organic acids, etc.) [18,19]. The obtained lignin bio-oils can be utilized in the production of resins, such as phenol-formaldehyde and epoxy resins, substituting petroleum-based phenols [24–27].

Alternatively, lignin bio-oils can be converted downstream into bio-/renewable fuels which can be used as blending components in bunker or aviation fuels [28,29]. Many attempts have been made to convert the light fractions of lignin bio-oils into aviation fuels, but the research is still mainly based on model phenolic monomers, dimers and surrogate mixtures, while a few researches are using real lignin bio-oils [30–32]. Furthermore, deep hydrodeoxygenation under more severe conditions can substantially decrease the oxygen content of bio-oil, leading to the formation of (alkyl)cycloalkanes and aromatics which can be utilized as drop-in aviation biofuels [32–39]. On the other hand, bunker fuels are based on heavy petroleum distillates and many feedstocks have been evaluated as blending components. Based on the goal of the International Maritime Organization to achieve a 70% reduction in carbon intensity in the shipping sector by 2050, low-sulfur and low-nitrogen fuels have been evaluated as bunker fuels [40]. Within this context, a wide variety of alternative feedstocks have been blended with standard marine diesel, such as oxymethylene ethers, fatty acid methyl esters, hydrotreated vegetable oils, Fischer–Tropsch fuels, hydrodeoxygenated pyrolysis oil, natural gas, liquified natural gas, liquified biogas and methanol [41–44]. The evaluation of these feedstocks has proved that they can be used in marine fuels without significant alterations to the properties of standard marine diesel or heavy oil fuel.

The aim of this work was to study the hydrotreatment of heavy fractions of lignin pyrolysis bio-oils under mild reaction conditions in terms of temperature, time and hydrogen pressure. The hydrotreatment was performed using two different alcohols (ethanol and methanol) as solvents and typical hydrogenolysis/hydrogenation (3%Ru/AC) and hydrogenation/hydrodeoxygenation (10%Ni/BETA) catalysts to induce hydrogenolysis of lignin oligomers to lower-molecular weight compounds and decrease the viscosity of bio-oils so that they could be incorporated as blending components in bunker fuels.

2. Materials and Methods

2.1. Lignin Pyrolysis Bio-Oil Production

Lignin pyrolysis bio-oil was obtained via the pyrolysis of Protobind 1000 lignin at a laboratory-scale fast pyrolysis unit in KIT. The pyrolysis experiments were performed in a fluidized bed reactor with a feeding capacity of 100 g/h, at 500 °C, under nitrogen flow and using sand as a heat carrier. The bio-oil was collected in two sequential condensers, which

were cooled to 60 and 0 °C to obtain a heavier organic condensate and a light aqueous condensate, respectively. The heavier fraction of lignin pyrolysis bio-oil collected at 60 °C was used for the hydrogenolysis experiments. A more detailed description of the pyrolysis unit is provided elsewhere [45]. The initial (received) bio-oil was a thick paste and kept at 4–8 °C.

2.2. Catalyst Synthesis and Characterization

Within this study, two different catalysts were used: a typical hydrogenation/hydrogenolysis catalyst (3% Ru/AC) and a bifunctional catalyst based on nickel supported on zeolite (10% Ni/BETA), which can induce hydrodeoxygenation reactions. The selection of metals and metal loading was based on previous studies, where 10 wt.% nickel on zeolite proved to be the optimum metal loading for achieving complete hydrodeoxygenation of model oxygenated phenolic and aromatic compounds [30]. Furthermore, the lower metal loading of ruthenium was selected based on its higher hydrogenation activity compared to that of transition metals, such as nickel, also with the aim of lowering the use of the less abundant ruthenium.

Via the wet impregnation method, 3% Ru/AC was prepared using $RuCl_3 \cdot xH_2O$ (99.9%; Strem Chemicals, Newburyport, MA, USA) as a ruthenium precursor and SAE Super (Cabot Norit SAE Super, Amsterdam, The Netherlands) as an activated carbon support. The pre-estimated amount of the precursor, corresponding to 3 wt.%, was dissolved in H_2O under stirring. After dilution, the solution was added dropwise into the aqueous suspension of activated carbon and stirring continued for 24 h. Afterwards, water was recovered and the solid was dried at 60 °C for 6 h under vacuum. Prior to the catalytic experiments, the catalyst was reduced at 350 °C for 1 h under 50 mL/min H_2 flow.

Then, 10% Ni/BETA was prepared via incipient dry impregnation using $Ni(NO_3)_2 \cdot 6H_2O$ (99.9%; ChemLab, Zedelgem, Belgium) as a nickel precursor and zeolite BETA (Si/Al = 12.5) as a catalyst support (Zeolyst, Conshohocken, PA, USA), which, prior to the impregnation, was calcined at 500 °C for 3 h to convert the ammonium form into the proton form. A specific amount of $Ni(NO_3)_2 \cdot 6H_2O$, corresponding to 10 wt.%, was dissolved in a certain amount of deionized water which corresponded to the total pore volume of the support. Afterwards, the aqueous solution was added slowly to the support and ground in a mortar. Then, the solid was dried at 100 °C and calcined at 500 °C for 3 h with a 2 °C/min heating rate. Prior to the catalytic experiments, the catalyst was reduced at 450 °C, for 3 h, under 50 mL/min H_2 flow.

The catalysts were characterized by X-Ray Powder Diffraction (XRD) and N_2 physisorption. XRD analysis was performed using a Rigaku Ultima+ 2cycles X-ray Diffractometer (Akishima, Japan) with CuKa X-ray radiation, over a $2\theta = 5$–85° range with 0.02°/step and 2 s/step. N_2 adsorption–desorption was performed at −196 °C using an Automatic Volumetric Sorption Analyzer (Autosorb-1 MP, Quantachrome, Boynton Beac, FL, USA). Prior to the measurements, the samples were outgassed at 250 °C for 19 h under 5×10^{-9} Torr vacuum. The total surface areas were determined via the multipoint BET method, and the total pore volume was determined at P/Po = 0.99. Micropore surface areas and volumes were determined via the t-plot method, while the mesopore size distributions were determined via the Barrett–Joyner–Halenda (BJH) method.

2.3. Hydrogenolysis of Lignin Pyrolysis Bio-Oil

Mild hydrotreatment/hydrogenolysis of the heavy fraction of lignin pyrolysis bio-oil was carried out in a high-temperature and high-pressure batch autoclave reactor equipped with a Parr 4848 controller (Parr, Moline, IL, USA). The lignin pyrolysis bio-oil (2 g) was dissolved in 20 mL methanol or ethanol and left under stirring overnight. After the addition

of the catalyst (3% Ru/AC or 10% Ni/BETA), at a catalyst-to-feed ratio (C/F) = 0.2, the reactor was flushed three times with hydrogen to remove air and a leak test was performed at 100 bar for 10 min. Afterwards, the reactor was pressurized with hydrogen at the selected pressure (30–50 bar H_2, room temperature) and the reaction was performed at 250 °C, for 1 h, with an agitation speed of approximately 400 rpm. After completion of the reaction, the reactor was rapidly cooled down to room temperature and gaseous products were collected in a vacuum bag for analysis. The catalyst was separated from the liquid product by vacuum filtration and dried at 80 °C for 6 h under vacuum conditions.

2.4. Characterization of Initial and Hydrotreated Bio-Oils

The initial lignin pyrolysis and the hydrotreated bio-oils were analyzed via GC-MS, using an Agilent 6890N-MSD 5973 GC-MS (Agilent, Palo Alto, CA, USA) equipped with an MXT-5 column (30 m × 0.25 mm × 0.25 μm, Restek, Bellefonte, PA, USA). The compound identification was based on NIST library.

Two-dimensional HSQC NMR spectra of bio-oils were obtained on a Varian (Agilent technologies, Santa Clara, CA, USA) 500 MHz DD2 spectrometer. Suitable amounts of lignin bio-oils were dissolved in 0.45 mL of DMSO-d_6 (99.8%; Deutero GmbH, Kastellaun, Germany) and stirred overnight. The chemical shifts were referenced to the solvent signal (2.500/39.520 ppm). The analysis parameters were set to 5 s relaxation delay, and spectral widths ranged from 13 to −1 ppm and from 160 to 0 ppm for the ^{1}H and ^{13}C dimensions, respectively. The spectra were processed using the MestReNova software (Version 14.0.2-26256). Prior to Fourier transformation, FID (free induction decay) signals were apodized with a $\pi/2$ sine squared bell function in both dimensions.

Water content was determined via Karl Fischer titration using the Karl Fisher volumetric titrator HI 903 (Hanna instruments, Bedfordshire, UK), Hydranal Water Standard 10.0 (Fluka, Seelze, Germany) and Hydranal Titrant 5 (Fluka, Seelze, Germany).

The stability of the bio-oils was examined via dynamic light scattering using an Anton Parr Litesizer 500 instrument (Anton Parr, Graz, Austria). The particle sizes of the bio-oils were measured using alcoholic suspensions with concentrations of 0.1–10 wt.% prepared under stirring.

Elemental composition and viscosity measurements was performed after the removal of solvents and water, first at room temperature and afterwards under vacuum conditions at 40 °C. The elemental composition of the bio-oils (C/H/N/S) was determined using the analyzer EA 3100 (EuroVector, Pavia, Italy). Viscosity measurements were performed using an MCR 302 rheometer (Anton Paar, Graz, Austria) equipped with a Peltier system at 50 °C, using a sheer stress of 6 1/s for all samples.

Molecular weight distributions (M_w and M_n) and the polydispersity (PDI) of the bio-oils were obtained by Gel Permeation Chromatography (GPC) using a Waters GPC instrument (Milford, MA, USA). The analysis was performed at 40 °C with a Waters 2414 refractive index detector (RID-10 A), two linear columns (Styragel HR4E, 5 μm, 7.8 mm × 300 mm, Waters, Milford, MA, USA) and tetrahydrofuran (THF) as an eluent at a flow rate of 1 mL/min. All samples were dissolved in THF (1 mg/mL) and filtered with a PTFE syringe filter (pore size 0.45 μm) prior to measurement. For the calibration lines, polystyrene standards were used within the calibration range of 162–204,000 Da.

2.5. Characterization of Spent Catalysts

Spent catalysts were characterized by various techniques to quantify coke and organics depositions, as well as to examine any changes in their structure. Carbon content was quantified via elemental analysis using the analyzer EA 3100 (EuroVector, Pavia, Italy). Coke depositions were also determined via thermogravimetric analysis using an STA

449 F5 Jupiter instrument (Netzsch, Selb, Germany). The analysis was performed in the temperature range of 25–950 °C under an air flow of 50 mL/min and with a heating rate of 10 °C/min.

3. Results

3.1. Characterization of Catalysts

The structure of the catalysts was determined via XRD analysis. In the XRD pattern of 3%Ru/AC, no peaks attributable to ruthenium structures (metals or oxides) were identified due to the high dispersion of ruthenium on the activated carbon, as can be observed in Figure 1a. Similar observations have been observed for other ruthenium catalysts supported on activated carbons or oxidic supports [46]. On the other hand, in the pattern of the 10%Ni/BETA catalysts, all the characteristic peaks of metallic nickel (Ni^0) were observed at 2θ = 44.5, 51.9 and 76.4°. The rest of the peaks were attributed to the BEA zeolite structure. The crystallite size of Ni^0, determined via the Scherrer equation, was found to be equal to 14 nm.
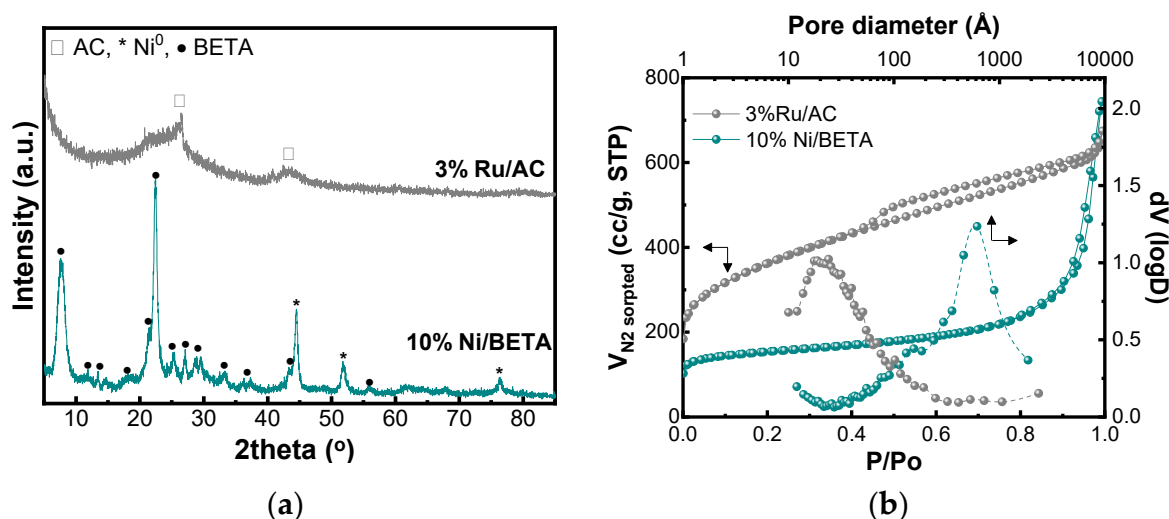
Figure 1. (**a**) XRD and (**b**) N_2 physisorption and BJH pore sizes distributions of the synthesized catalysts.

The two supports used exhibit distinct porous and acidic properties. Regarding the porous properties, the catalyst 3%Ru/AC exhibits a micro-/mesoporous structure with a combination of Type I and IV isotherms, according to the IUPAC classification (Figure 1b). The surface area calculated via the linear BET equation was found to be equal to 1263 m^2/g, and the total pore volume was 0.826 cm^3/g. The microporous area was determined via the t-plot method, and it was found to be 494 m^2/g, which demonstrates that 39% of the porosity is attributable to micropores, while 61% is attributable to mesopores and the external surface area (Table 1). Similar properties were observed for the catalyst 10%Ni/BETA, which exhibited a combination of Type I and Type IV isotherms with a H4 hysteresis loop (Figure 1b), corresponding to microporous materials with enhanced meso-/macroporous characteristics. The surface area was 562 m^2/g, almost half that of the 3%Ru/AC, while the total pore volume was higher and equal to 1.151 cm^3/g. The microporous area was found to be 371 m^2/g, which demonstrates that 66% of the porosity is attributable to micropores and that the rest (44%) is attributable to meso-/macropores and the external surface area. However, a clear difference between the two support materials is the average mesopore size, with carbon exhibiting substantially smaller micropores (2.4 nm) compared to those of BETA zeolite (62 nm).

Table 1. Physicochemical characterization of catalysts.

Catalysts	$D_{crystallite}$ (nm)	S_{BET} (m^2/g)	S_{micro} (m^2/g)	S_{meso} (m^2/g)	V_{total} (cm^3/g)	V_{micro} (cm^3/g)	$D_{pore, BJH}$ (nm)
3%Ru/AC	<3	1263	494	769	0.826	0.232	2.4
10%Ni/BETA	14	562	371	191	1.151	0.154	62

3.2. Mild Hydrogenolysis of Lignin Pyrolysis Bio-Oils

Prior to the hydrotreatment of lignin pyrolysis bio-oil, its solubility in alcohols was examined via particle size distribution measurements. As can be observed in the particle size distributions of Figure 2a,b, the solubility of bio-oil is strongly dependent on its concentration, as well as on the type of alcohol. The lower concentration of 0.1 wt.% is fully solubilized in both methanol and ethanol, as can be observed in the insert photographs of Figure 2. The particles exhibit very small diameters, 0.61 and 0.66 μm, in ethanol and methanol, respectively. An increase in bio-oil concentration to 1 wt.% led to an increase in particle diameters to 1.49 and 2.10 μm in ethanol and methanol, respectively. A further increase in concentration to 10 wt.% limited the solubility, and the diameters of the particles increased to 14.35 and 10.90 μm in ethanol and methanol. The particle diameters exhibited almost a linear correlation with the concentration of bio-oils and more specifically were based on the equation d = 1.10·concentration for methanol and d = 1.44·concentration for ethanol. Additionally, the limited solubility of the bio-oil at the highest concentration (10 wt.%) resulted in depositions on the walls of the vials, as shown in the insert photographs of Figure 2. Another parameter studied via DLS was the stability of the (hydro)treated bio-oils. After hydrogenolysis in methanol at 250 °C, for 1 h and under 30 bar H$_2$, particles were still observed, but they were substantially smaller (0.54 μm), with a narrower particle size distribution, indicating enhanced depolymerization of the initial bio-oil (Figure 2c). The size of the particles remained stable after 17 days (0.50 μm), proving that the hydrotreated bio-oils are stable.
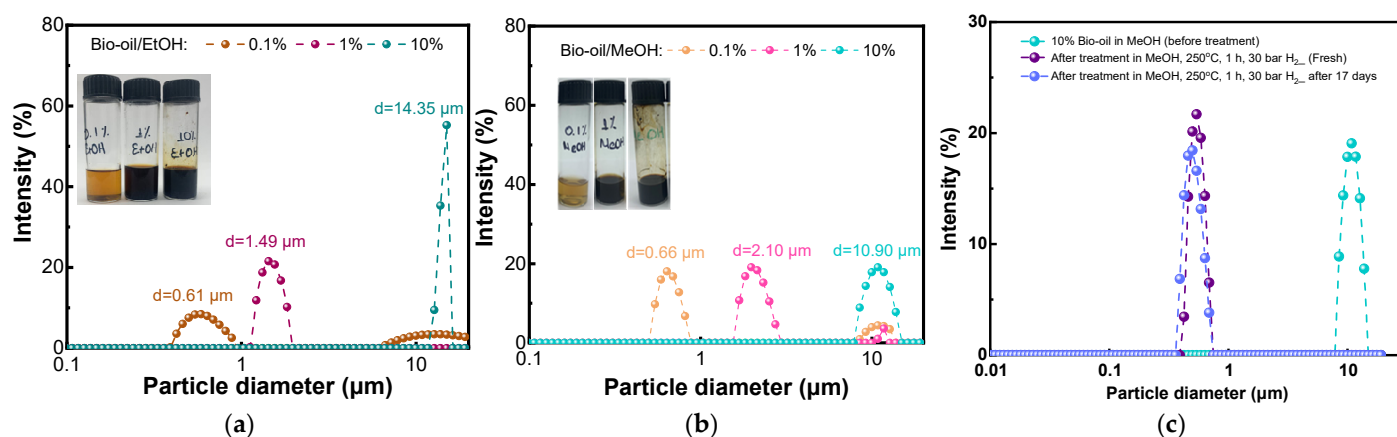

Figure 2. Particle size distributions of the lignin pyrolysis bio-oil dissolved in (**a**) ethanol and (**b**) methanol and (**c**) after (hydro)treatment.

3.2.1. Bio-Oil and Gaseous Product Yields

Despite the limited solubility of the 10 wt.% bio-oil in both alcohols, the hydrotreatment experiments were carried out with this concentration at 250 °C, for 1 h, using 3%Ru/AC and 10%Ni/BETA. Using neat ethanol, without a catalyst and without hydrogen gas, the solvolysis of lignin oligomers led to the recovery of 46 wt.% liquid bio-oil, while the char formed in the bottom of the reactor was 23 wt.%, as can be observed in Figure 3, while no gaseous products were formed. The addition of 30 bar hydrogen gas

(initial pressure at room temperature) increased the bio-oil yield to 64 wt.%, while the char was decreased to 17 wt.%, proving that the hydrogen pressure had a beneficial effect. When 3%Ru/AC was used as a typical hydrogenation/hydrogenolysis catalyst, the cleavage of inter-unit linkages between lignin monomers/oligomers was enhanced, resulting in a decrease in the bio-oil yield to 38 wt.% and a further decrease in the coke/char yield to 12 wt.%, but a substantial increase in gaseous products to 4.7 wt.%. On the other hand, the addition of the 10%Ni/BETA catalyst led to a similar bio-oil yield (61 wt.%) and coke/char yield (13 wt.%) compared to the non-catalytic solvolysis. The concentration of gases were also very low with this catalyst (0.5 wt.%). Additionally, the zeolite support enhanced the dehydration reactions, which increased the water yield to 2.4 wt.%. Compared to the experiments carried out with ethanol as a solvent, the hydrotreatments in methanol led to lower bio-oil yields and higher coke/char yields. More specifically, in neat methanol, under 30 bar H_2 (initial pressure), the solvolysis experiment led to a 56 wt.% bio-oil yield, a 24 wt.% char yield and a 0.7 wt.% gas yield. The addition of 10%Ni/BETA under the same hydrogen initial pressure slightly decreased the bio-oil yield to 48 wt.% and coke formation to 19 wt.%, along with a small increase in the water content. An increase in hydrogen pressure from 30 bar to 50 bar had no beneficial effect in terms of enhancing the bio-oil yield (Figure 3).
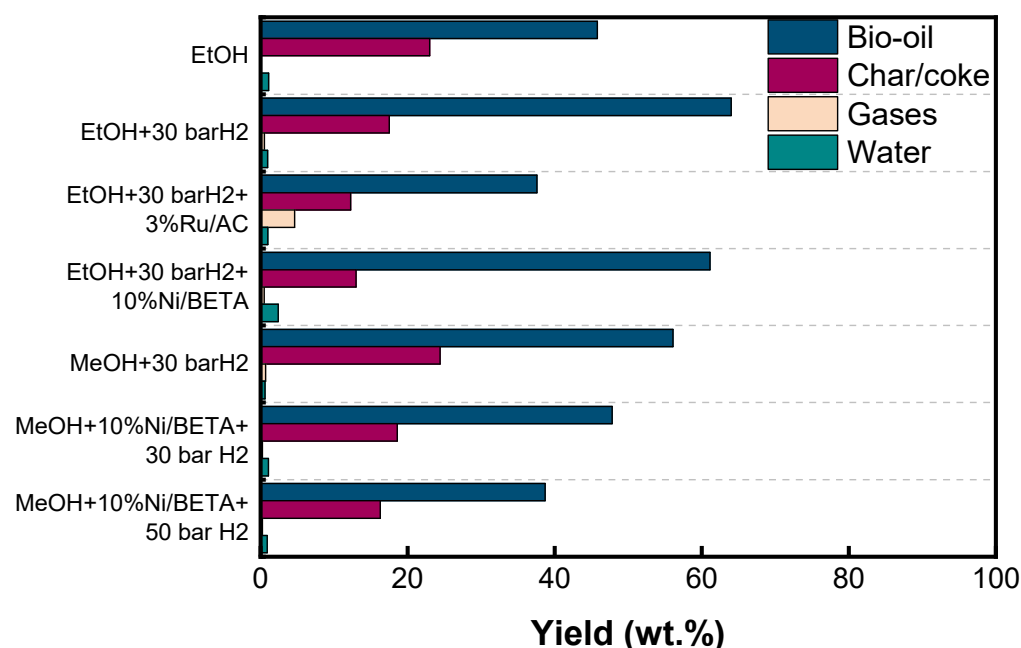

Figure 3. Yields of liquid bio-oil, char/coke, gases and water produced during the (hydro)treatment of lignin pyrolysis bio-oils at 250 °C, 1 h.

Regarding the gaseous product analysis, the treatment in ethanol under 30 bar H_2 led to the formation of carbon dioxide, carbon monoxide and methane, formed upon partial decarbonylation/decarboxylation and demethylation of phenolic compounds (Figure 4). The addition of 3%Ru/AC led to a partial decrease in carbon dioxide from 0.5 wt.% to 0.3 wt.% and an increase in carbon monoxide to 2.6 wt.% and methane to 1.4 wt.%. Also, the hydrogenolysis occurred in the presence of 3%Ru/ACled to the formation of propane (0.03 wt.%), propylene (0.03 wt.%) and C_{5+}/C_{6+} hydrocarbons (0.3 wt.%). As a result, the catalyst 3%Ru/AC enhanced the decarbonylation, demethylation and dealkylation reactions instead of decarboxylation, which mainly occurred in the solvolysis experiment. Furthermore, the addition of 10%Ni/BETA led to lower carbon dioxide concentrations and higher carbon monoxide concentrations, compared to the solvolysis experiments. The acid

sites of the BETA zeolite induced partial hydrocracking towards C_{5+}/C_{6+} and propylene. In the solvolysis experiments carried out in methanol, the most abundant gas was carbon monoxide, showing that decarbonylation reactions are favored in methanol compared to ethanol. The addition of 10% Ni/BETA (12.5) catalysts led to a decrease in carbon monoxide and increases in carbon dioxide, C_{5+}/C_{6+} and methane. An increase in hydrogen pressure from 30 to 50 bar slightly decreased the yields of methane, C_{5+}/C_{6+} and carbon monoxide and increased the yield of carbon dioxide. The complete gas analysis is shown in Figure 4.
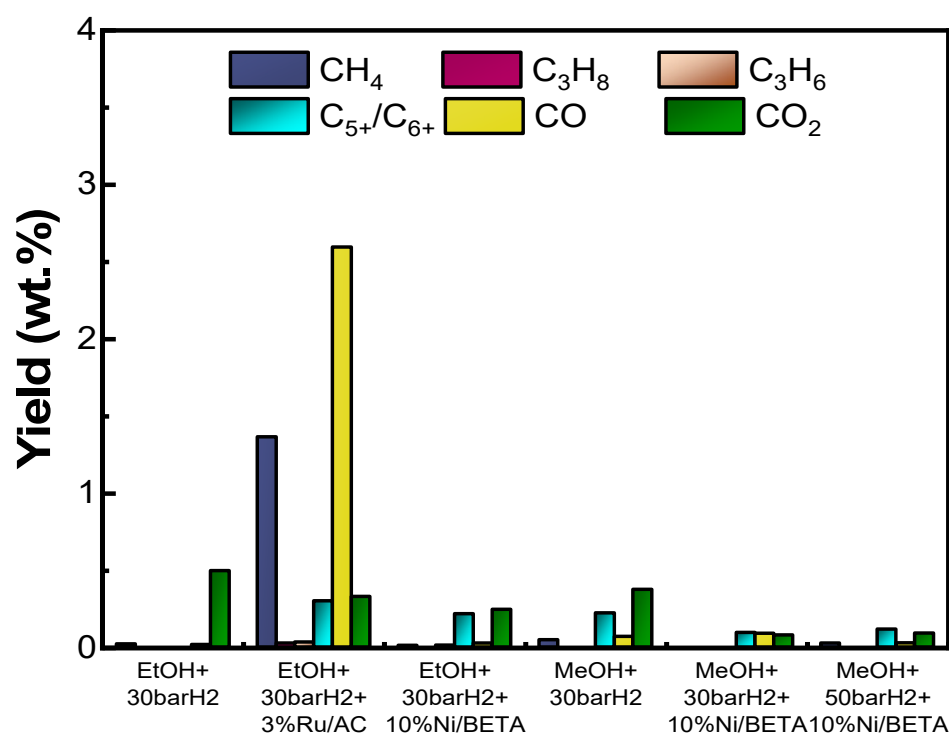
Figure 4. Analysis of the gases produced during the (hydro)treatment of lignin bio-oils.

3.2.2. Analysis of Bio-Oil Compositions

The compositions of the (hydro)treated bio-oils were determined via GC-MS analysis, and the identified compounds were grouped in the categories shown in Figure 5; the five most abundant compounds in each bio-oil are shown in Tables 2 and 3. The initial lignin pyrolysis bio-oil exhibited a high relative concentration of oxygenated phenols (OxyPH, 50.8%), followed by nitrogen-containing compounds (NIT, 11.1%), alkylated phenols (PH, 9.1%), furanic compounds (FUR, 5.4%), polycyclic aromatic hydrocarbons (PAH, 5.3%) and carboxylic acids (AC, 4.2%), while compounds in the rest of the categories were identified at lower concentrations (<3%). Focusing on the oxygenated phenols, they were substituted with one and two methoxy groups due to the hardwood nature of the lignin, which was derived from wheat straw and sarkansa bagasse. Furthermore, compounds such as ketones, acids and furanics are formed upon the pyrolysis of sugar impurities which remain after alkaline pulping to isolate lignin.
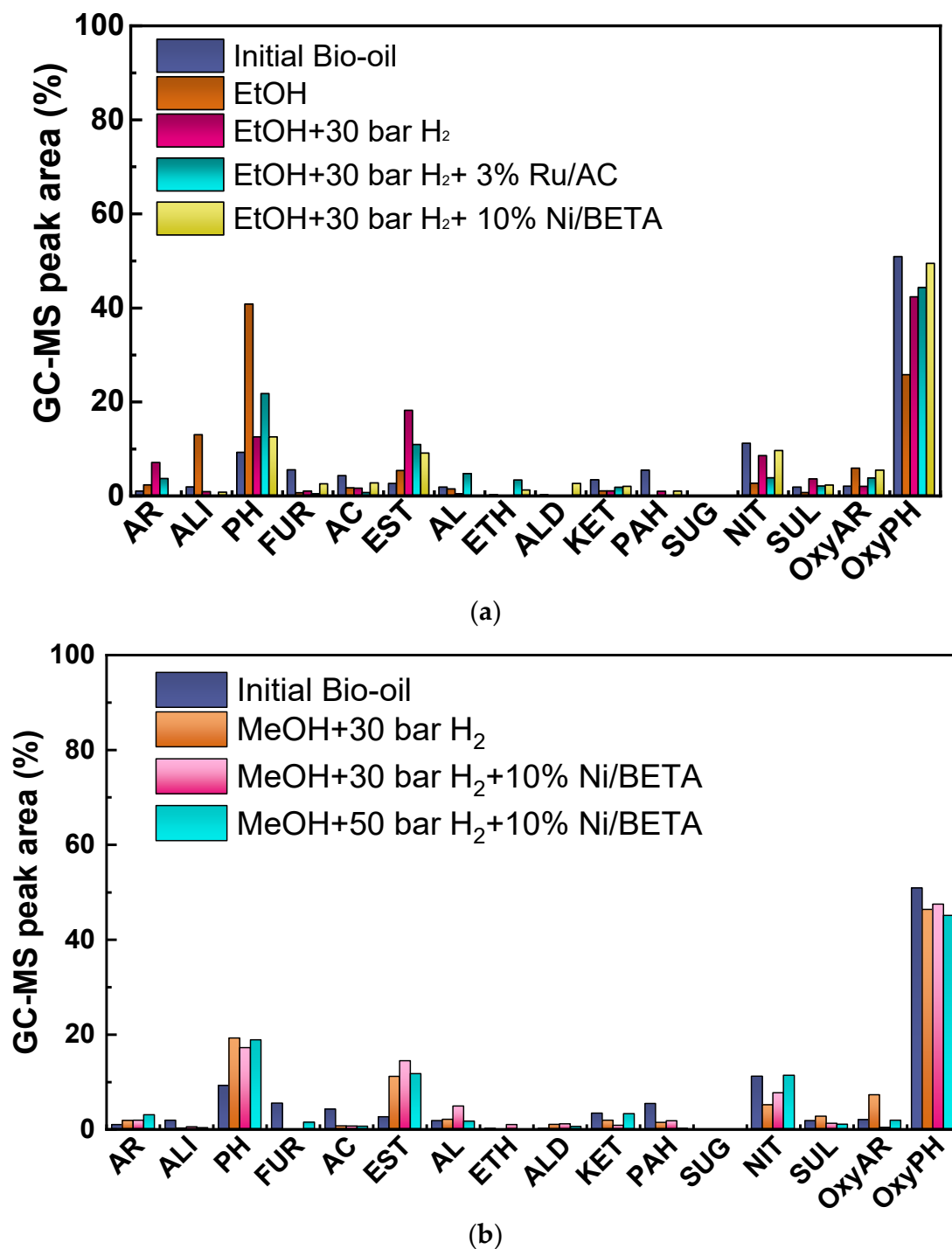
Figure 5. Compounds identified in the GC-MS analysis of the various (hydro)treated Protobind lignin pyrolysis bio-oils in (**a**) ethanol and (**b**) methanol. AR—aromatics, ALI—aliphatics, PH—alkylated phenols, FUR—furanics, AC—acids, EST—esters, AL—alcohols, ETH—ethers, ALD—aldehydes, KET—ketones, PAH—polycyclic aromatic hydrocarbons, SUG—sugars, NIT—nitrogen-containing compounds, SUL—sulfur-containing compounds, OxyAR—oxygenated aromatics, OxyPH—alkoxylated phenols, UN—unknown compounds.

Table 2. Five most abundant compounds identified via GC-MS analysis in the initial lignin pyrolysis bio-oil and the (hydro)treated bio-oils in ethanol.
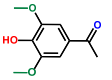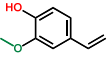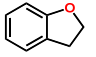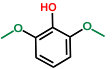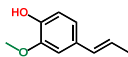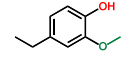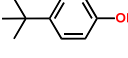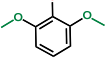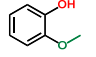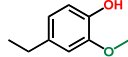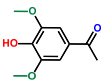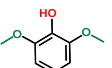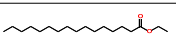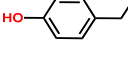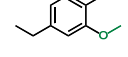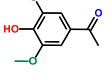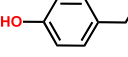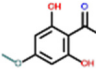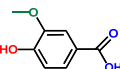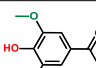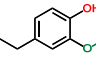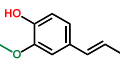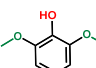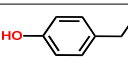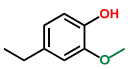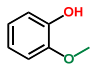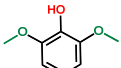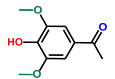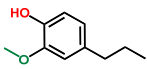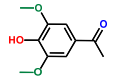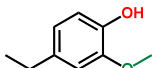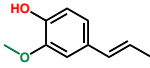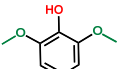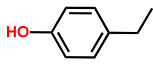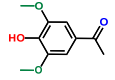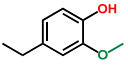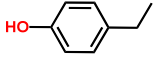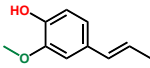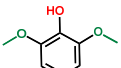
Compound	Category	Structure	Relative Abundance (%)
Initial bio-oil			
Ethanone, 1-(4-hydroxy-3,5-dimethoxyphenyl)-	OxyPH		12.1
2-Methoxy-4-vinylphenol	OxyPH		8.1
Benzofuran, 2,3-dihydro-	FUR		4.6
Phenol, 2,6-dimethoxy-	OxyPH		4.4
Phenol, 2-methoxy-4-(1-propenyl)-, (E)-	OxyPH		3.9
Critical/supercritical EtOH solvolysis			
Phenol, 4-ethyl-2-methoxy-	OxyPH		5.9
Eicosane	ALI		5.6
Phenol, p-tert-butyl-	PH		4.7
Phenol, 2,6-dimethoxy-	OxyPH		3.7
Phenol, 2-methoxy-	OxyPH		3.7
EtOH + 30 bar H_2			
Phenol, 4-ethyl-2-methoxy-	OxyPH		9.1
Ethanone, 1-(4-hydroxy-3,5-dimethoxyphenyl)-	OxyPH		7.1
Phenol, 2,6-dimethoxy-	OxyPH		6.8
Hexadecanoic acid, ethyl ester	EST		6.1
Phenol, 4-ethyl-	PH		5.3
EtOH + 30 bar H_2+ 3%Ru/AC			
Phenol, 4-ethyl-2-methoxy-	OxyPH		9.2
Ethanone, 1-(4-hydroxy-3,5-dimethoxyphenyl)-	OxyPH		6.4
Phenol, 4-ethyl-	PH		5.8

Table 2. *Cont.*

Compound	Category	Structure	Relative Abundance (%)
EtOH + 30 bar H$_2$+ 3%Ru/AC			
Ethanone, 1-(2,6-dihydroxy-4-methoxyphenyl)-	OxyPH		4.8
Benzoic acid, 4-hydroxy-3-methoxy-	OxyPH		4.4
EtOH + 30 bar H$_2$+ 10% Ni/BETA			
Ethanone, 1-(4-hydroxy-3,5-dimethoxyphenyl)-	OxyPH		10.6
Phenol, 4-ethyl-2-methoxy-	OxyPH		8.8
Phenol, 2-methoxy-4-(1-propenyl)-, (E)-	OxyPH		5.1
Phenol, 2,6-dimethoxy-	OxyPH		5.0
Phenol, 4-ethyl-	PH		4.9

The treatment (solvolysis) in neat ethanol at critical conditions (almost supercritical conditions, the critical temperature of ethanol being 241 °C), without the addition of hydrogen gas or a catalyst, led to a significant decrease in the relative concentration of alkoxylated phenols (OxyPH) from 50.8% in the initial lignin pyrolysis bio-oil to 25.7%. On the other hand, the relative abundance of alkylated phenols (PH) increased from 9.1% to 40.7%, both the above results being indicative of the thermal dealkoxylation reaction which occurred during the solvolysis process at critical ethanol conditions. Also, after this intensive solvolysis treatment, the relative concentrations of aromatics (BTX and dimers), aliphatic compounds (linear alkanes) and fatty acids/esters existing in the lignin pyrolysis oil increased. The addition of 30 bar H$_2$, still a without catalyst, led to a somewhat lower dealkoxylation of alkoxy-phenols and an increase in alkylated phenols (i.e., OxyPH decreased from 50.8% in the initial lignin pyrolysis bio-oil to 42.2% and PH increased from 9.1% to 12.4%), due to minimization of the critical/supercritical conditions of ethanol upon initial pressurization with H$_2$. Furthermore, under hydrogen pressure, an increase in the monoaromatic compounds (alkylated substituted biphenyl) concentration from 0.9% to 6.9% was observed. Interestingly, the addition of 30 bar H$_2$ also enhanced the esterification reactions of the fatty acids and the carboxylic acids of the bio-oils with the solvent towards the formation of the respective ethyl esters with C$_{16}$-C$_{26}$ carbon numbers. The formation of esters is desirable because it can stabilize a bio-oil and prevent its self-polymerization [47]. Apart from the formation of esters, the consumption of ethanol during the non-catalytic treatment was almost negligible due to the mild reaction temperature. According to studies in the literature on non-catalytic solvolysis of lignins, alcohol consumption is 10–35 wt.% in the temperature range of 300–400 °C towards carbon monoxide, water and esters, such as ethyl acetate, ethers, etc. [48]. The experiments of the current study were conducted below or close to the critical point, which limited the solvent cracking even more.

Table 3. Five most abundant compounds identified via GC-MS analysis in the (hydro)treated bio-oils in methanol.

Compound	Category	Structure	Relative Abundance (%)
MeOH + 30 bar H$_2$			
Phenol, 4-ethyl-2-methoxy-	OxyPH		10.1
Phenol, 2-methoxy-	OxyPH		8.8
Phenol, 2,6-dimethoxy-	OxyPH		7.6
Ethanone, 1-(4-hydroxy-3,5-dimethoxyphenyl)-	OxyPH		4.3
Phenol, 2-methoxy-4-propyl-	OxyPH		3.7
MeOH + 30 bar H$_2$+ 10%Ni/BETA			
Ethanone, 1-(4-hydroxy-3,5-dimethoxyphenyl)-	OxyPH		11.6
Phenol, 4-ethyl-2-methoxy-	OxyPH		6.6
Phenol, 2-methoxy-4-(1-propenyl)-, (E)-	OxyPH		4.8
Phenol, 2,6-dimethoxy-	OxyPH		4.4
Phenol, 4-ethyl-	PH		4.4
MeOH + 50 bar H$_2$+ 10%Ni/BETA			
Ethanone, 1-(4-hydroxy-3,5-dimethoxyphenyl)-	OxyPH		9.3
Phenol, 4-ethyl-2-methoxy-	OxyPH		8.4
Phenol, 4-ethyl-	PH		5.2
Phenol, 2-methoxy-4-(1-propenyl)-, (E)	OxyPH		4.8
Phenol, 2,6-dimethoxy-	OxyPH		4.1

Using methanol as a solvent, the experiment with under 30 bar H$_2$ induced partial thermal dealkoxylation of oxygenated phenols to alkyl-phenolic compounds, whose concentration increased from 9.1% in the initial bio-oil to 19.2% in the treated bio-oil and was slightly enhanced compared to when ethanol was used as the solvent. The concentration of

oxygenated aromatics also increased from 1.9% in the initial bio-oil to 7.2%. Comparing the two experiments with the two solvents under 30 bar hydrogen, minor differences were observed in the composition of the bio-oils in methanol and ethanol, except in the case of aromatics and esters, which were more abundant in the ethanol-treated bio-oil.

Regarding the catalytic hydrotreatment in ethanol, the addition of 3%Ru/AC induced hydrogenolysis of lignin oligomers towards fragments of lower molecular weight, as well as dealkoxylation of oxygenated phenols to alkylated phenols (their relative concentration increased from 12.4% to 21.6%) and oxygenated aromatics, whose concentration increased from 1.9 to 3.7%. Despite the higher concentration of alkylated phenols, the concentration of oxygenated phenols was almost similar (44.2%) to that of those in the critical ethanol-treated bio-oil (42.2%), most probably due to enhanced hydrogenolysis of larger oligomers (not identifiable via GC-MS) towards the formation of smaller (monomer) oxygenated phenols. Furthermore, the use of the 3%Ru/AC limited the esterification reaction of acids with the solvent, and thus the concentration of esters decreased to 10.8% from 18.1% in the non-catalytic ethanol-treated bio-oil. Another important effect of the catalyst's addition was the decrease in the relative concentrations of nitrogen- and sulfur-containing compounds to 3.7% and 1.9%, respectively, compared to the ethanol-treated bio-oil (8.5% and 3.5%) and the initial pyrolysis bio-oil (11.1% and 1.7%), which is beneficial for their evaluation as bio-/renewable fuels. Also, compared to the initial lignin pyrolysis bio-oil, the hydrotreatment with 3% Ru/AC increased the relative concentration of aromatics from 0.9% to 3.5% and that of esters from 2.5% to 10.8%.

The hydrotreatment in ethanol with 10%Ni/BETA (12.5) maintained the high relative concentrations of both OxyPH and alkylated phenols compared to the non-catalytic ethanol-treated bio-oil under 30 bar H_2. The nickel–zeolite catalyst limited the esterification reaction of acids with the solvent, and consequently the relative concentration of esters was significantly lower, 8.9% instead of 18.1%, in the ethanol-treated bio-oil. On the other hand, the relative concentration of oxygenated aromatics increased from 1.9% in the ethanol-treated bio-oil to 5.3%. Compared to hydrotreatment with 3%Ru/AC, the bifunctional nickel–zeolite catalyst led to significantly lower concentrations of alkylated phenols (12.4% instead of 21.6% with the 3%Ru/C catalyst) and lower concentrations of aromatics (negligible formation). Also, the hydrotreatment with 10%Ni/BETA led to a limited decrease in nitrogen- and sulfur-containing compounds (9.5% and 2.2%) compared to the enhanced performance of 3%Ru/AC.

Among the two solvents (ethanol and methanol) used with 10% Ni/BETA, methanol led to higher concentrations of alkylated phenols (17.2% instead of 12.4%), esters (14.4% instead of 8.9%) and alcohols, while ethanol led to higher concentrations of aliphatics, acids, furanics, oxygenated aromatics and oxygenated phenols. Finally, the increase in hydrogen pressure from 30 to 50 bar in the hydrotreatment with methanol and 10% Ni/BETA did not have significant effects on the composition of the hydrotreated bio-oil, as can be observed in Figure 5b. The main differences between the two experiments were the slightly higher concentration of aromatics (3.0% at 50 bar instead of 1.8% at 30 bar) and the lower concentration of esters (11.6% at 50 bar instead of 14.4% at 30 bar). The five most abundant compounds identified in all the treated bio-oils are shown in Tables 2 and 3. As can be observed in both tables, the oxygenated phenols were the most abundant compounds in almost all the samples, while furanic compounds, fatty esters and alkylated phenols were also found at significant concentrations.

Further elucidation of the composition of the bio-oil samples was performed via 2D HSQC NMR analysis, and the spectra are shown in Figures 6–8. In the initial bio-oil derived via the pyrolysis of Protobind lignin, signals corresponding to oxygenated phenolic compounds were observed in the aromatic region (δ_C/δ_H = 95-140/5.6-8.1) as

well as at δ_C/δ_H = 95-140/3.1-4.2, corresponding to methoxy groups. The aromatic units consisted of both syringyl ($S_{2,6}$ and $S'_{2,6}$ in oxidized C_a = O) and guaiacyl units (G_2, G'_2 and G_5) due to the hardwood nature of the lignin, while H-units were less abundant ($H_{2,6}$). The S/G/H ratio was estimated to be 41/45/13. Furthermore, cross peaks corresponding to ortho-, meta- or para-substituted phenols were observed in the aliphatic region (δ_C/δ_H = 5-45/0-2.6). Also, in this region, signals corresponding to unsaturated fatty acids were identified at δ_C/δ_H = 28-32/1.0-1.3 ppm. Regarding the inter-unit linkages, in the region δ_C/δ_H = 60-95/2.5-6.0 ppm, the most abundant linkages (β-β, β-5 and β-O-4) were absent due to their cleavage during lignin pyrolysis, and only traces of 4-O-5 ether bonds were observed at δ_C/δ_H = 106-110/6.4-6.5 ppm.

The solvolysis that occurred under critical/supercritical ethanol conditions (in the absence of catalyst and H_2) induced the dealkoxylation of oxygenated phenolics towards alkylated phenols, as can be observed by the substantially smaller cross peaks of the S- and G-groups and the higher intensity of the H-groups, as well as the lower signals of methoxy groups at δ_C/δ_H = 95-140/3.1-4.2 (Figure 6). The NMR analysis data were in accordance with the GC-MS results, both giving a S/G/H ratio of about 10/41/49. Also, the signal corresponding to 4-O-5 ether bonds is absent from the spectrum of the treated bio-oil, which confirms the further cleavage of inter-unit linkages under these solvolysis/critical conditions in ethanol. On the other hand, the signals corresponding to the cross peaks of aliphatic compounds are increased, which is indicative of the higher concentrations of alkylated phenols and linear alkanes, as was also observed in the GC-MS analysis. The addition of hydrogen gas (30 bar H_2) during the ethanol treatment of the bio-oil (in the absence of catalyst) enhanced the depolymerization of lignin oligomers towards monomers, as can be observed via the more intense signals of S-, G- and H-units at δ_C/δ_H = 95-140/5.6-8.1 and of methoxy groups at δ_C/δ_H = 95-140/3.1-4.2, compared to the solvolysis experiment without the addition of hydrogen gas. The S/G/H ratio was found to be equal to 29/37/34. In the catalytic hydrotreatment experiments, a considerable decrease in the signals corresponding to the methoxy-, S- and G-derived compounds was observed compared to both the initial bio-oil and the solvolysis products (Figure 7). On the contrary, the signals of the compounds with terminal methyl groups and the alkyl groups of phenols became more intense. The S/G/H ratios were estimated to be 22/45/33 using 3%Ru/AC and 27/51/22 for 10%Ni/BETA, which confirms the higher selectivity of the ruthenium catalyst towards the cleavage of ether linkages as well as the enhanced dealkoxylation activity.

Regarding the treatment of bio-oil in methanol (under an initial pressure of 30 bar H_2), the signals of the compounds were less intense compared to those observed in the experiments performed in ethanol (Figure 8a). More specifically, the cross peaks of oxygenated phenolics with S-, G- and H-groups exhibited lower intensities at δ_C/δ_H = 95-140/3.1-4.2, and the estimated S/G/H ratio was 28/36/36, almost similar to the ratio obtained using ethanol. The use of 10%Ni/BETA as a hydrotreatment catalyst did not significantly change the 2D HSQC NMR spectra of the product (Figure 8b). The main difference was the absence of a cross peak at δ_C/δ_H = 60-65/3.6-4.8, which was attributed to the aromatic alcohols. The increase in hydrogen pressure from 30 bar to 50 bar H_2 also had a slight influence on the composition of the hydrotreated bio-oil (Figure 8c). In accordance with the GC-MS analysis, the main differences in the NMR spectra were the more intense peaks of S- and G-units at δ_C/δ_H = 95-140/5.6-8.1, which led to the S/G/H ratio of 27/45/28.
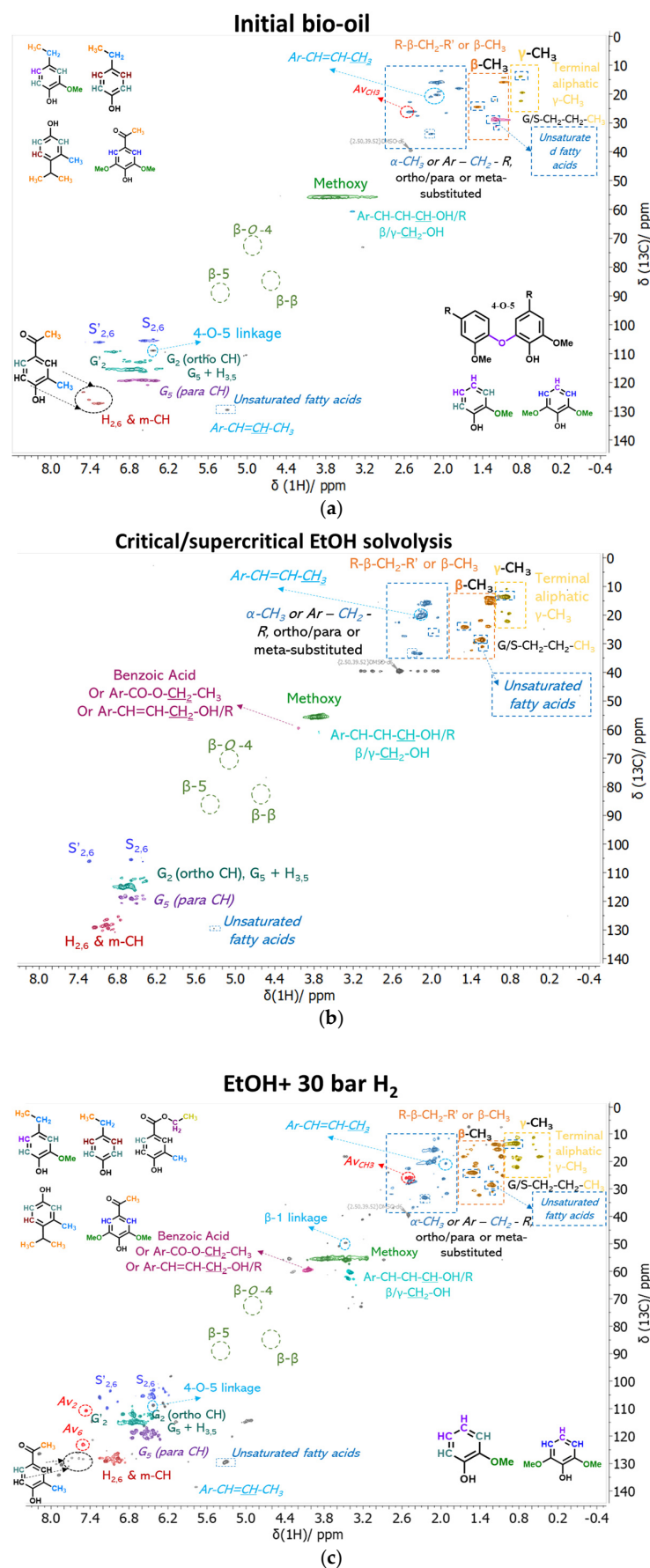
Figure 6. Two-dimensional HSQC NMR spectra of the (**a**) initial and (**b**,**c**) treated lignin pyrolysis bio-oils in ethanol.

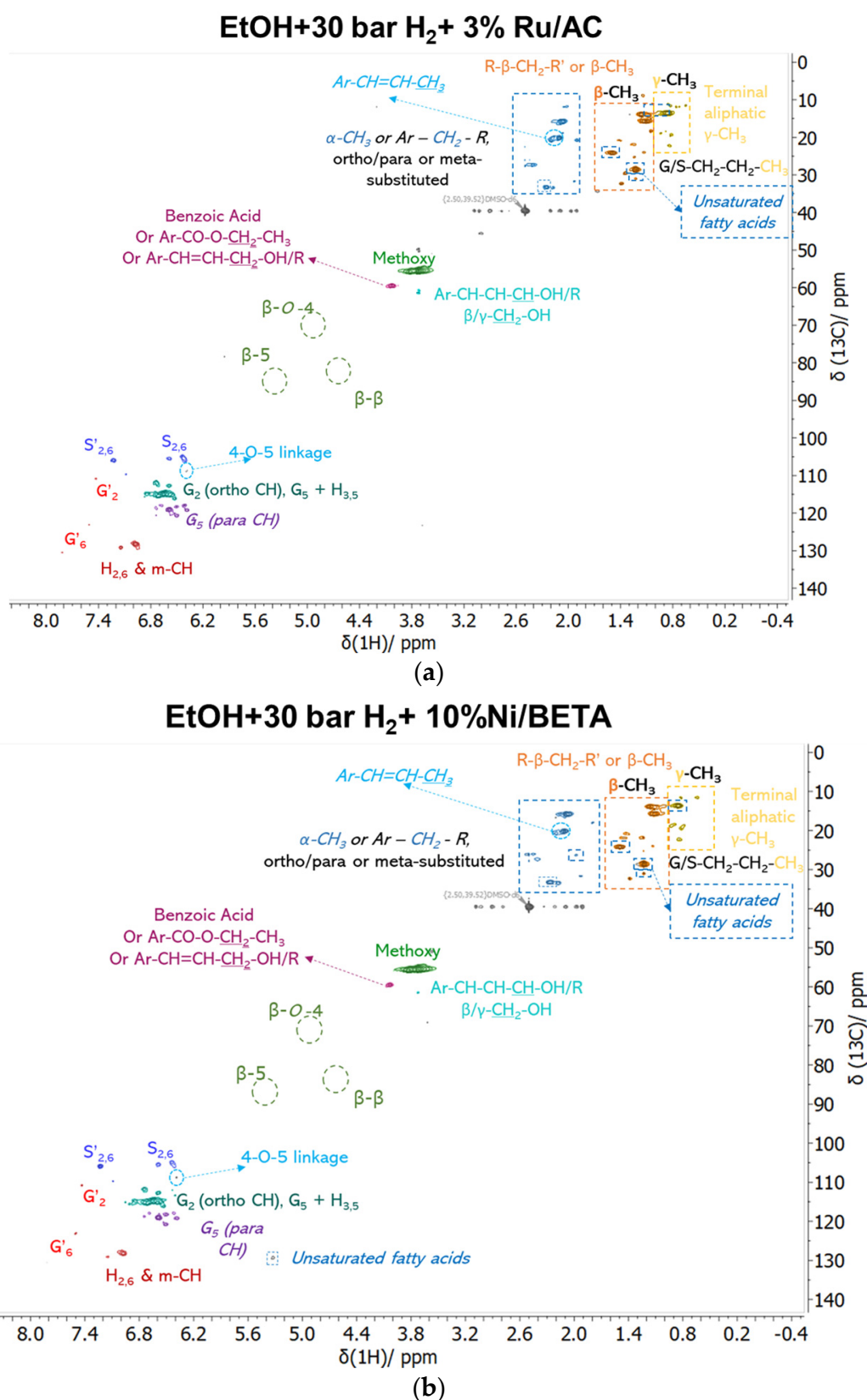**Figure 7.** Two-dimensional HSQC NMR spectra of the hydrotreated lignin pyrolysis bio-oils in ethanol using (**a**) 3%Ru/AC and (**b**) 10%Ni/BETA.
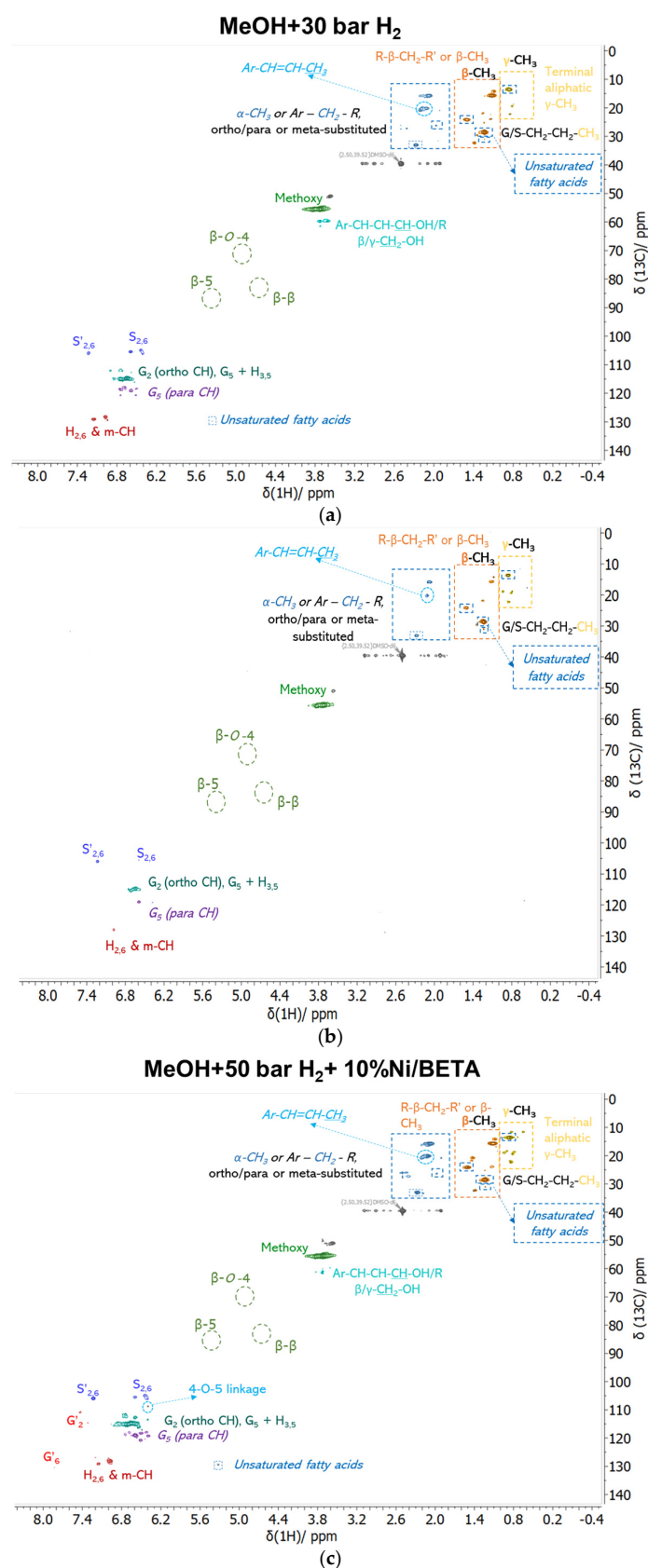
Figure 8. Two-dimensional HSQC NMR spectra of the (hydro)treated lignin pyrolysis bio-oils in methanol: (**a**) non-catalytic experiment, (**b**) using 10%Ni/BETA+ 30 bar H_2 and (**c**) using 10%Ni/BETA+ 50 bar H_2.

3.2.3. Evaluation of Bio-Oil Properties

After the removal of solvents, the (hydro)treated bio-oils (i.e., after solvolysis or catalytic hydrotreatment) were characterized via elemental analysis to determine the carbon, hydrogen, nitrogen, sulfur and oxygen contents (Table 4). All (hydro)treated bio-oils exhibited high carbon contents in the range 62.9–73.2%, hydrogen contents in the range of 6.8–8.0% and very low nitrogen contents in the range 0.6–0.9%, and they were sulfur-free. It is important to highlight the absence of sulfur, which is preferred regarding potential valorization as a drop-in bunker fuel. The oxygen content, determined via difference, ranged between 17.9% and 29.7%. In the solvolysis experiments, performed in ethanol or methanol, the treated bio-oils exhibited higher carbon contents and lower oxygen contents than the initial bio-oil or the bio-oils produced via the catalytic hydrotreatment. These results were in accordance with the GC-MS and the NMR analyses, where the partial deoxygenation was confirmed for the solvolysis experiments. The higher carbon content of the bio-oils treated in alcohols (under solvolysis conditions) were in accordance with similar studies in the literature. Furthermore, it was suggested that the increase in the organic chain length of the alcohol leads to an increase in the carbon content of the treated bio-oil, as was also observed in the present study [49]. On the other hand, all the catalytic hydrotreatments using either 3%Ru/AC or 10%Ni/BETA led to lower carbon and higher oxygen contents, possibly due to enhanced hydrogenolysis of larger condensed oligomers to phenolic monomers, as discussed above. Interestingly, all the (hydro)treated bio-oils exhibited higher hydrogen contents (7.1–8.0 wt.%) compared to the initial bio-oil (7.1 wt.%). Furthermore, the calculation of the atomic O/C and H/C ratios led to the Van Krevelen diagram of Figure 9, and the calorific values of the (hydro)treated bio-oils were higher than those of the parent lignocellulosic biomass or the initial Protobind lignin and very close to those of lignite. The same trend was observed via the calculation of a higher heating value (HHV), shown in Table 4. The values were calculated on the basis of the elemental analysis data and according to the method mentioned in [50]. The treated bio-oils exhibited HHVs in the range of 27.2–33.5 MJ/kg, while the bio-oils obtained via the solvolysis of lignin pyrolysis bio-oils exhibited higher values compared to the initial pyrolysis bio-oil and the catalytic hydrotreated bio-oils.
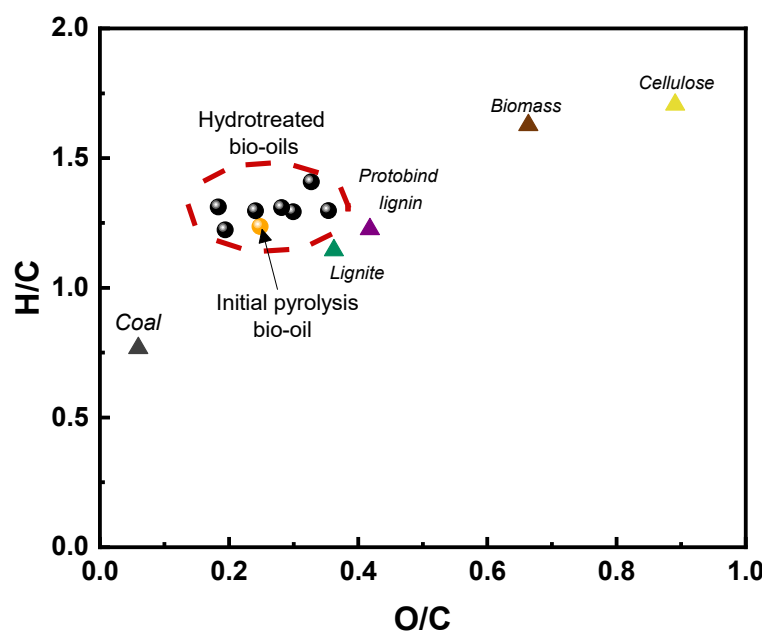

Figure 9. Van Krevelen diagram of the initial and the (hydro)treated lignin pyrolysis bio-oils, compared to fossil and lignocellulosic biomass fractions.

After the dilution of (hydro)treated bio-oils in tetrahydrofuran (THF), GPC analysis was performed for the determination of the molecular weights, and the results are shown in Table 4. It can be seen that pyrolysis of P1000 lignin provided a bio-oil with a much lower average molecular weight (M_w = ~570 g/mol) compared to that of parent P1000, as expected. The molecular weights of the treated bio-oil samples were somehow increased, and the samples treated at 250 °C and 30 bar H_2 with methanol or ethanol as a solvent and without catalysts exhibited molecular weights of 1200–1700 g/mol, indicating a slight repolymerization/condensation under these conditions towards bigger fragments, similar to the reductive depolymerization of lignins [51,52]. Among the two solvents, methanol resulted in lower molecular weights compared to ethanol. When a catalyst was used, e.g., 3%Ru/AC or 10%Ni/BETA, the molecular weight was decreased again, to 750–1100 g/mol, due to the hydrogenolysis action of the catalysts that inhibited/counterbalanced the above identified condensation of the phenolics in the bio-oil.

The most profound effect of the bio-oil's treatment was the tremendous decrease in viscosity, as can be observed in Table 4. The initial lignin pyrolysis bio-oil exhibited a viscosity equal to 298,147 cP, while the solvolysis in neat ethanol decreased the viscosity to 1500–1800 cP. The catalytic hydrogenolysis with 3% Ru/C reduced the viscosity further to 1276 cP, as can be seen in Table 4. The lowest viscosity (526 cP) was achieved via hydrotreatment with 10%Ni/BETA in methanol at 50 bar H_2. Kim et al. reported a decrease in the viscosity of Kraft lignin pyrolysis bio-oil from 751 to 20 cP via solvent-free hydrocracking at 400 °C using sulfided CoMo/Hβ catalysts and mentioned that the less viscous product can be more easily and effectively used as a feedstock in continuous-flow hydrodeoxygenation [53]. Furthermore, aging of pyrolysis oil–alcohol mixtures at 200 °C for 50 h showed a significant reduction in viscosity, which is beneficial for their stabilization and further hydrotreatment [54].

Table 4. Properties of initial and (hydro)treated lignin pyrolysis bio-oils.

Reaction Conditions	C [1] (wt.%)	H [1] (wt.%)	N [1] (wt.%)	S [1] (wt.%)	O [2] (wt.%)	HHV [3] (MJ/kg)	M_n (g/mol)	M_w (g/mol)	PDI	Viscosity (cP)
Protobind lignin	59.7	6.1	0.9	~0	33.3	24.9	1746 [4]	2987 [4]	1.7 [4]	-
Initial bio-oil	68.9	7.1	1.2	~0	22.8	30.5	245	572	2.3	298,147
EtOH solvolysis	73.2	8.0	0.9	~0	17.9	33.5	335	816	2.4	1778
EtOH + 30 bar H_2	72.6	7.4	1.2	~0	18.8	32.5	428	1738	4.1	1500
EtOH + 30 bar H_2+ 3% Ru/AC	63.9	7.5	0.7	~0	27.9	28.5	341	832	2.4	1276
EtOH + 30 bar H_2+ 10% Ni/BETA	65.9	7.1	0.7	~0	26.3	29.0	377	1096	2.9	4439
MeOH + 30 bar H_2	69.4	7.5	0.8	~0	22.3	31.1	434	1247	2.9	2625
MeOH + 30 bar H_2+ 10% Ni/BETA	66.9	7.3	0.7	~0	25.1	29.7	211	744	3.5	8273
MeOH + 50 bar H_2+ 10% Ni/BETA	62.9	6.8	0.6	~0	29.7	27.2	368	982	2.7	526

[1] Determined via elemental analysis (±0.2%). [2] Determined via difference: 100-C(%)-H(%)-N(%). [3] Determined via elemental analysis according to [50]. [4] The molecular weight of Protobind lignin was obtained in ref. [55].

3.3. Characterization of Char and Spent Catalysts

Apart from the analysis of the bio-oils, a characterization of the used catalysts and the formed chars was also performed. Regarding the non-catalytic experiments, i.e., in the absence of catalysts, the char formed due to the repolymerization of monomers/oligomers led to a solid with a high carbon content in the range of 70.7–85.4 wt.%, with the highest amount observed in the char isolated via solvolysis under critical conditions (Table 5).

The high carbon content was also confirmed via TGA analysis. As can be observed in Figure 10a, the char obtained via the critical–ethanol solvolysis experiment exhibited one decomposition step in the temperature range of 420–560 °C (T_{max} = 480 °C), higher than the decomposition of the char isolated via the treatment in ethanol under 30 bar H_2. The latter exhibited a lower carbon content (70.7 wt.%) and decomposed in the temperature range of 360–480 °C (T_{max} = 430 °C), which is indicative of the less condensed nature of the carbonaceous solid. On the other hand, the spent 10%Ni/BETA catalyst exhibited several weight-loss steps. The total weight loss was 32.9 wt.% and was achieved in three distinct steps. The first step with a weight loss of 3.6 wt.% in the range 62–175 °C (T_{max} = 59 °C) is attributable to the removal of solvent impurities. The second weight loss (22.9 wt.%) within the temperature range of 175–450 °C (T_{max} = 322 °C) was mainly due to the burning of light organic compounds or the light coke, while the third step at 450–660 °C (T_{max} = 510 °C) was due to the burning of more condensed coke. The higher decomposition temperature of coke is indicative of its higher molecular weight, despite the lower carbon content (13.4 wt.%) compared to the char formed upon the treatment in neat ethanol.

Table 5. Physicochemical characterization of chars and spent catalysts.

Solid	Reaction Conditions	D_{XRD} (nm)	C (wt.%)	H (wt.%)	N (wt.%)	S (wt.%)	O (wt.%)
Char	EtOH	-	85.4	4.8	0.8	0.0	9.0
Char	EtOH + 30 bar H_2	-	70.7	4.8	2.3	0.0	22.1
Catalyst	EtOH + 30 bar H_2+ 3% Ru/AC	-	4.1	1.9	0.4	0.0	93.6
Catalyst	EtOH + 30 bar H_2+ 10% Ni/BETA	15	13.4	1.9	0.7	0.0	84.0
Char	MeOH + 50 bar H_2	-	77.7	5.8	1.2	0.0	15.3
Catalyst	MeOH + 30 bar H_2+ 10% Ni/BETA	15	35.1	3.5	1.2	0.1	60.0
Catalyst	MeOH + 50 bar H_2+ 10% Ni/BETA	16	27.8	3.2	1.1	0.1	67.8
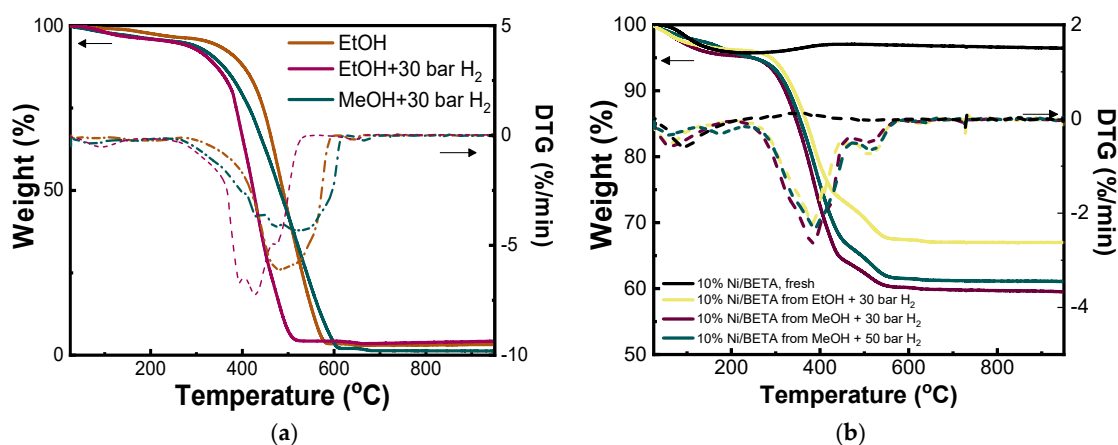
Figure 10. Thermogravimetric analysis of (**a**) chars recovered from the non-catalytic treatment of lignin bio-oils and (**b**) spent catalysts recovered from the hydrotreatment using 10%Ni/BETA.

Similarly, the char formed during the treatment in methanol with 30 bar H_2 exhibited a high carbon content (77.7 wt.%), slightly higher than the carbon content of the char formed during the same experiment with ethanol. That result was also confirmed via the thermogravimetric analysis. The char decomposed in one step at higher temperatures 240–700 °C (T_{max} = 517 °C), and the total weight loss was 94.0 wt.%. Furthermore, the char/coke deposits on the 10%Ni/BETA catalysts were 27.8–35.1 wt.%, significantly higher

than the value for the char/coke formed during the hydrotreatment in ethanol but lower than the one obtained after the treatment in neat methanol in the absence of a catalyst. The increase in the hydrogen pressure from 30 to 50 bar H_2 limited the coke formation on the catalyst. As can be observed in the TGA analysis of Figure 10b, the char from the experiment with 30 bar H_2 was decomposed in three steps. In the first step, 24–200 °C (T_{max} = 65 °C), the removal of the solvent led to a weight loss of 4.7 wt.%. At higher temperatures of 210–470 °C (T_{max} = 386 °C), the burning of light organics and light coke led to a weight loss of 32 wt.%, while an extra weight loss (3.9 wt.%) at 470–670 °C (T_{max} = 506 °C) corresponded to the burning of heavier coke. The main difference with the catalysts recovered via the experiment under 50 bar H_2 was the lower total weight loss of that catalyst, possibly due to the lower carbon content. Despite the lower amount of carbon depositions, the coke had a "harder" (more condensed) nature, leading to a higher weight loss (5 wt.%) in the temperature range of 470–670 °C (T_{max} = 517 °C).

Despite the carbon depositions on the catalysts, the metallic phases of the catalysts were maintained, as confirmed via XRD analysis of the used catalysts. In the XRD pattern for 3% Ru/AC, shown in Figure 11a, the uniform dispersion of ruthenium was maintained without any agglomeration towards bigger crystallites or the oxidation towards ruthenium oxide formation. Similarly, all the used 10%Ni/BETA catalysts recovered from the ethanol and methanol hydrotreatments seemed to maintain the metallic phase of nickel, as can be observed in Figure 11b, and the characteristic reflections at 2θ = 44.5, 51.9 and 76.3°.
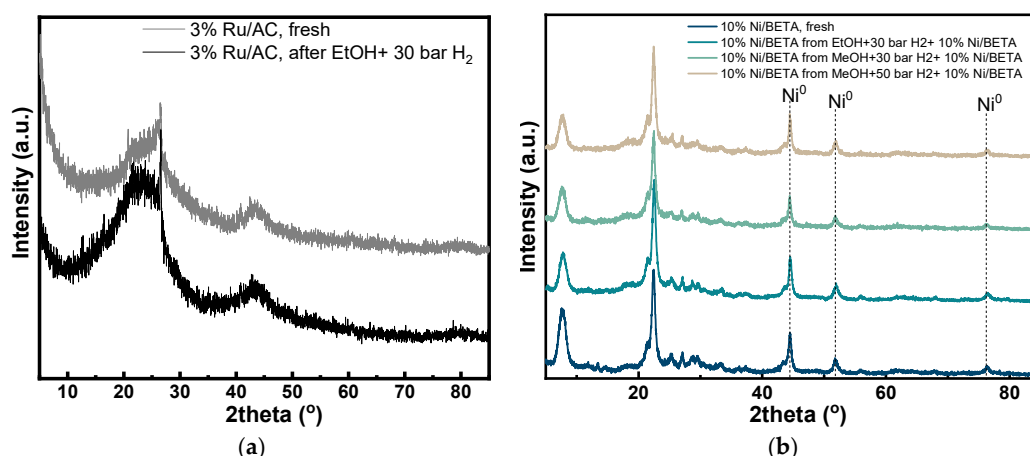

Figure 11. XRD patterns of spent (**a**) 3%Ru/AC and (**b**) 10%Ni/BETA catalysts.

4. Conclusions

The aim of this work was to develop a mild hydrotreatment for heavy organic condensates (bio-oils) produced via the fast pyrolysis of lignin. The hydrotreatment was performed using simple alcohols (methanol or ethanol) as solvents and typical hydrogenolysis (3%Ru/AC) and hydrogenation/hydrodeoxygenation (10%Ni/BETA) catalysts under mild reaction conditions (250 °C, 1 h). The possible contribution of the hydrogen-donor effect of these alcohols/solvents was not examined in this work, as externally added H_2 gas at 30–50 bar (the initial pressure at ambient conditions) was used in all the catalytic hydrogenolysis experiments. Solvolysis experiments under critical or subcritical conditions were also performed and proved to be very effective, at least in terms of deoxygenating the existing smaller (monomer) phenolics in the lignin pyrolysis oil. On the other hand, the catalytic hydrotreatment enhanced the hydrogenolysis of lignin oligomers towards the lower-molecular weight compounds via the cleavage of C-C and ether inter-unit linkages. Furthermore, in all cases, partial dealkoxylation of alkoxy-phenols was enhanced towards alkylated phenols and aromatics. The formation of esters was also observed and

is beneficial for the stabilization of bio-oil. The most noticeable effect was the decrease in viscosity, which can facilitate not only the handling of bio-oil during blending with conventional bunker fuels, but also its potential downstream deep hydrodeoxygenation towards aromatic/cycloalkane hydrocarbons.

References

1. Hong, J.; Chen, B.; Wang, T.; Zhao, X. A promising technical route for converting lignocellulose to bio-jet fuels based on bioconversion of biomass and coupling of aqueous ethanol: A techno-economic assessment. *Fuel* **2025**, *381*, 133670. [CrossRef]
2. Ashokkumar, V.; Venkatkarthick, R.; Jayashree, S.; Chuetor, S.; Dharmaraj, S.; Kumar, G.; Chen, W.-H.; Ngamcharussrivichai, C. Recent advances in lignocellulosic biomass for biofuels and value-added bioproducts—A critical review. *Bioresour. Technol.* **2022**, *344*, 126195. [CrossRef] [PubMed]
3. Liu, W.-J.; Yu, H.-Q. Thermochemical Conversion of Lignocellulosic Biomass into Mass-Producible Fuels: Emerging Technology Progress and Environmental Sustainability Evaluation. *ACS Environ. Au* **2022**, *2*, 98–114. [CrossRef] [PubMed]
4. Thoresen, P.P.; Matsakas, L.; Rova, U.; Christakopoulos, P. Recent advances in organosolv fractionation: Towards biomass fractionation technology of the future. *Bioresour. Technol.* **2020**, *306*, 123189. [CrossRef]
5. Tofani, G.; Jasiukaitytė-Grojzdek, E.; Grilc, M.; Likozar, B. Organosolv biorefinery: Resource-based process optimisation, pilot technology scale-up and economics. *Green Chem.* **2024**, *26*, 186–201. [CrossRef]
6. Margellou, A.G.; Psochia, E.A.; Torofias, S.A.; Pappa, C.P.; Triantafyllidis, K.S. Isolation of Highly Crystalline Cellulose via Combined Pretreatment/Fractionation and Extraction Procedures within a Biorefinery Concept. *ACS Sustain. Resour. Manag.* **2024**, *1*, 1432–1443. [CrossRef]
7. Kammoun, M.; Margellou, A.; Toteva, V.B.; Aladjadjiyan, A.; Sousa, A.F.; Luis, S.V.; Garcia-Verdugo, E.; Triantafyllidis, K.S.; Richel, A. The key role of pretreatment for the one-step and multi-step conversions of European lignocellulosic materials into furan compounds. *RSC Adv.* **2023**, *13*, 21587–21612. [CrossRef]
8. Lu, X.; Gu, X. A review on lignin-based epoxy resins: Lignin effects on their synthesis and properties. *Int. J. Biol. Macromol.* **2023**, *229*, 778–790. [CrossRef]
9. Pappa, C.P.; Torofias, S.; Triantafyllidis, K.S. Sub-Micro Organosolv Lignin as Bio-Based Epoxy Polymer Component: A Sustainable Curing Agent and Additive. *ChemSusChem* **2023**, *16*, e202300076. [CrossRef]
10. Gioia, C.; Colonna, M.; Tagami, A.; Medina, L.; Sevastyanova, O.; Berglund, L.A.; Lawoko, M. Lignin-Based Epoxy Resins: Unravelling the Relationship between Structure and Material Properties. *Biomacromolecules* **2020**, *21*, 1920–1928. [CrossRef]
11. Pang, B.; Yang, S.; Fang, W.; Yuan, T.-Q.; Argyropoulos, D.S.; Sun, R.-C. Structure-property relationships for technical lignins for the production of lignin-phenol-formaldehyde resins. *Ind. Crops Prod.* **2017**, *108*, 316–326. [CrossRef]
12. Gaudenzi, E.; Cardone, F.; Lu, X.; Canestrari, F. The use of lignin for sustainable asphalt pavements: A literature review. *Constr. Build. Mater.* **2023**, *362*, 129773. [CrossRef]
13. Domínguez-Robles, J.; Cárcamo-Martínez, Á.; Stewart, S.A.; Donnelly, R.F.; Larrañeta, E.; Borrega, M. Lignin for pharmaceutical and biomedical applications—Could this become a reality? *Sustain. Chem. Pharm.* **2020**, *18*, 100320. [CrossRef]
14. Alqahtani, M.S.; Alqahtani, A.; Al-Thabit, A.; Roni, M.; Syed, R. Novel lignin nanoparticles for oral drug delivery. *J. Mater. Chem. B* **2019**, *7*, 4461–4473. [CrossRef]
15. Abu-Omar, M.M.; Barta, K.; Beckham, G.T.; Luterbacher, J.S.; Ralph, J.; Rinaldi, R.; Román-Leshkov, Y.; Samec, J.S.M.; Sels, B.F.; Wang, F. Guidelines for performing lignin-first biorefining. *Energy Environ. Sci.* **2021**, *14*, 262–292. [CrossRef]
16. Renders, T.; Van den Bosch, S.; Koelewijn, S.F.; Schutyser, W.; Sels, B.F. Lignin-first biomass fractionation: The advent of active stabilisation strategies. *Energy Environ. Sci.* **2017**, *10*, 1551–1557. [CrossRef]
17. Renders, T.; Van den Bossche, G.; Vangeel, T.; Van Aelst, K.; Sels, B. Reductive catalytic fractionation: State of the art of the lignin-first biorefinery. *Curr. Opin. Biotechnol.* **2019**, *56*, 193–201. [CrossRef]

18. Wang, S.; Li, X.; Ma, R.; Song, G. Catalytic Hydrogenolysis of Lignin into Serviceable Products. *Acc. Chem. Res.* **2025**, *58*, 529–542. [CrossRef]

19. Margellou, A.; Triantafyllidis, K.S. Catalytic Transfer Hydrogenolysis Reactions for Lignin Valorization to Fuels and Chemicals. *Catalysts* **2019**, *9*, 43. [CrossRef]

20. Liu, X.; Bouxin, F.P.; Fan, J.; Budarin, V.L.; Hu, C.; Clark, J.H. Recent Advances in the Catalytic Depolymerization of Lignin towards Phenolic Chemicals: A Review. *ChemSusChem* **2020**, *13*, 4296–4317. [CrossRef]

21. Charisteidis, I.; Lazaridis, P.; Fotopoulos, A.; Pachatouridou, E.; Matsakas, L.; Rova, U.; Christakopoulos, P.; Triantafyllidis, K. Catalytic Fast Pyrolysis of Lignin Isolated by Hybrid Organosolv—Steam Explosion Pretreatment of Hardwood and Softwood Biomass for the Production of Phenolics and Aromatics. *Catalysts* **2019**, *9*, 935. [CrossRef]

22. Margellou, A.G.; Lazaridis, P.A.; Charisteidis, I.D.; Nitsos, C.K.; Pappa, C.P.; Fotopoulos, A.P.; Van den Bosch, S.; Sels, B.F.; Triantafyllidis, K.S. Catalytic fast pyrolysis of beech wood lignin isolated by different biomass (pre)treatment processes: Organosolv, hydrothermal and enzymatic hydrolysis. *Appl. Catal. A-Gen.* **2021**, *623*, 118298. [CrossRef]

23. Soldatos, P.; Margellou, A.; Pappa, C.; Torofias, S.; Matsakas, L.; Rova, U.; Christakopoulos, P.; Triantafyllidis, K. Conversion of beechwood organosolv lignin via fast pyrolysis and in situ catalytic upgrading towards aromatic and phenolic-rich bio-oil. *Sustain. Chem. Environ.* **2024**, *6*, 100107. [CrossRef]

24. Pappa, C.; Feghali, E.; Vanbroekhoven, K.; Triantafyllidis, K.S. Recent advances in epoxy resins and composites derived from lignin and related bio-oils. *Curr. Opin. Green Sustain. Chem.* **2022**, *38*, 100687. [CrossRef]

25. Vithanage, A.E.; Chowdhury, E.; Alejo, L.D.; Pomeroy, P.C.; DeSisto, W.J.; Frederick, B.G.; Gramlich, W.M. Renewably sourced phenolic resins from lignin bio-oil. *J. Appl. Polym. Sci.* **2017**, *134*, 44827. [CrossRef]

26. Agbo, P.; Mali, A.; Deng, D.; Zhang, L. Bio-Oil-Based Epoxy Resins from Thermochemical Processing of Sustainable Resources: A Short Review. *J. Compos. Sci.* **2023**, *7*, 374. [CrossRef]

27. Chaouch, M.; Diouf, P.N.; Laghdir, A.; Yin, S. Bio-oil from whole-tree feedstock in resol-type phenolic resins. *J. Appl. Polym. Sci.* **2014**, *131*, 40014. [CrossRef]

28. Saidi, M.; Moradi, P. Chapter 3—Conversion of lignin-derived bio-oil to bio-jet fuel. In *Sustainable Alternatives for Aviation Fuels*; Yousuf, A., Gonzalez-Fernandez, C., Eds.; Elsevier: Amsterdam, The Netherlands, 2022; pp. 49–68.

29. Kong, X.; Liu, C.; Fan, Y.; Li, M.; Xiao, R. Enhanced Upgrading of Crude Lignin Bio-Oil to Jet Fuel Precursors with a Moderate Organic Acid-Modified Copper Catalyst. *ACS Sustain. Chem. Eng.* **2023**, *11*, 7454–7465. [CrossRef]

30. Zormpa, F.F.; Margellou, A.G.; Karakoulia, S.A.; Delli, E.; Triantafyllidis, K.S. Hydrodeoxygenation of lignin bio-oil model compounds and surrogate mixtures over zeolite supported nickel catalysts. *Catal. Today* **2024**, *433*, 114654. [CrossRef]

31. Margellou, A.G.; Zormpa, F.F.; Karfaridis, D.; Karakoulia, S.A.; Triantafyllidis, K.S. Hydrodeoxygenation of Phenolic Compounds and Lignin Bio-Oil Surrogate Mixture over Ni/BEA Zeolite Catalyst and Investigation of Its Deactivation. *Catalysts* **2025**, *15*, 48. [CrossRef]

32. Luo, Z.; Liu, C.; Radu, A.; de Waard, D.F.; Wang, Y.; Behaghel de Bueren, J.T.; Kouris, P.D.; Boot, M.D.; Xiao, J.; Zhang, H.; et al. Carbon–carbon bond cleavage for a lignin refinery. *Nat. Chem. Eng.* **2024**, *1*, 61–72. [CrossRef]

33. Duan, H.; Dong, J.; Gu, X.; Peng, Y.-K.; Chen, W.; Issariyakul, T.; Myers, W.K.; Li, M.-J.; Yi, N.; Kilpatrick, A.F.R.; et al. Hydrodeoxygenation of water-insoluble bio-oil to alkanes using a highly dispersed Pd–Mo catalyst. *Nat. Commun.* **2017**, *8*, 591. [CrossRef] [PubMed]

34. Fu, Z.-P.; Zhou, Q.-J.; Zhao, Y.-P.; Wu, Y.-F.; Liu, F.-J.; Zhong, M.; Li, J.; Liang, J.; Cao, J.-P. Selective hydrodeoxygenation of guaiacol and bio-oil to cycloalkanes over Ni-based catalysts supported on altered Hβ zeolite. *Mol. Catal.* **2025**, *576*, 114932. [CrossRef]

35. Kumar, A.; Khani, Y.; Ko, C.H.; Jae, J.; Banerjee, A.; Bhaskar, T.; Park, Y.-K. Production of Valuable Aromatics from the Hydrodeoxygenation of Guaiacol and Real Bio-Oil over Ni–Nb/HZSM-5 under Supercritical Ethanol. *ACS Sustain. Chem. Eng.* **2024**, *12*, 10786–10804. [CrossRef]

36. Li, B.-S.; Feng, B.-X.; Wu, K.-Y.; Yang, T.-H. Hydrodeoxygenation of lignin derived bio-oil into aromatic hydrocarbons over Ni-Cu-Ru/HZSM-5 catalyst. *J. Fuel Chem. Technol.* **2023**, *51*, 358–365. [CrossRef]

37. Li, L.; Huang, Z.; Shu, F.; Gao, Y.; Long, J. Hydrodeoxygenation of heavy lignin bio-oil to oxygenated fuel catalyzed by CuxNiy/MgO. *Fuel* **2024**, *357*, 129805. [CrossRef]

38. Shu, R.; Li, R.; Lin, B.; Wang, C.; Cheng, Z.; Chen, Y. A review on the catalytic hydrodeoxygenation of lignin-derived phenolic compounds and the conversion of raw lignin to hydrocarbon liquid fuels. *Biomass Bioenergy* **2020**, *132*, 105432. [CrossRef]

39. Ismail, O.; Hamid, A.; Ali, L.; Shittu, T.; Kuttiyathil, M.S.; Iqbal, M.Z.; Khaleel, A.; Altarawneh, M. Selective formation of fuel BXT compounds from catalytic hydrodeoxygenation of waste biomass over Ni-decorated beta-zeolite. *Bioresour. Technol. Rep.* **2023**, *24*, 101616. [CrossRef]

40. International Maritime Organization. Initial IMO strategy on reduction of GHG emissions from ships. In *Resolution MEPC*; International Maritime Organization: London, UK, 2018; Volume 304.

41. Bullermann, J.; Meyer, N.-C.; Krafft, A.; Wirz, F. Comparison of fuel properties of alternative drop-in fuels with standard marine diesel and the effects of their blends. *Fuel* **2024**, *357*, 129937. [CrossRef]

42. Hansson, J.; Månsson, S.; Brynolf, S.; Grahn, M. Alternative marine fuels: Prospects based on multi-criteria decision analysis involving Swedish stakeholders. *Biomass Bioenergy* **2019**, *126*, 159–173. [CrossRef]

43. Zhang, Z.; E, J.; Deng, Y.; Pham, M.; Zuo, W.; Peng, Q.; Yin, Z. Effects of fatty acid methyl esters proportion on combustion and emission characteristics of a biodiesel fueled marine diesel engine. *Energy Convers. Manag.* **2018**, *159*, 244–253. [CrossRef]

44. Masum, F.H.; Zaimes, G.G.; Tan, E.C.D.; Li, S.; Dutta, A.; Ramasamy, K.K.; Hawkins, T.R. Comparing Life-Cycle Emissions of Biofuels for Marine Applications: Hydrothermal Liquefaction of Wet Wastes, Pyrolysis of Wood, Fischer–Tropsch Synthesis of Landfill Gas, and Solvolysis of Wood. *Environ. Sci. Technol.* **2023**, *57*, 12701–12712. [CrossRef] [PubMed]

45. Funke, A.; Tomasi Morgano, M.; Dahmen, N.; Leibold, H. Experimental comparison of two bench scale units for fast and intermediate pyrolysis. *J. Anal. Appl. Pyrolysis* **2017**, *124*, 504–514. [CrossRef]

46. Lazaridis, P.A.; Karakoulia, S.A.; Teodorescu, C.; Apostol, N.; Macovei, D.; Panteli, A.; Delimitis, A.; Coman, S.M.; Parvulescu, V.I.; Triantafyllidis, K.S. High hexitols selectivity in cellulose hydrolytic hydrogenation over platinum (Pt) vs. ruthenium (Ru) catalysts supported on micro/mesoporous carbon. *Appl. Catal. B-Environ.* **2017**, *214*, 1–14. [CrossRef]

47. Reyhanitash, E.; Tymchyshyn, M.; Yuan, Z.; Albion, K.; van Rossum, G.; Xu, C. Hydrotreatment of fast pyrolysis oil: Effects of esterification pre-treatment of the oil using alcohol at a small loading. *Fuel* **2016**, *179*, 45–51. [CrossRef]

48. Nielsen, J.B.; Jensen, A.; Schandel, C.B.; Felby, C.; Jensen, A.D. Solvent consumption in non-catalytic alcohol solvolysis of biorefinery lignin. *Sustain. Energy Fuels* **2017**, *1*, 2006–2015. [CrossRef]

49. Shafaghat, H.; Lee, I.-G.; Jae, J.; Jung, S.-C.; Park, Y.-K. Pd/C catalyzed transfer hydrogenation of pyrolysis oil using 2-propanol as hydrogen source. *Chem. Eng. J.* **2019**, *377*, 119986. [CrossRef]

50. Mateus, M.M.; Bordado, J.M.; Galhano dos Santos, R. Estimation of higher heating value (HHV) of bio-oils from thermochemical liquefaction by linear correlation. *Fuel* **2021**, *302*, 121149. [CrossRef]

51. Kouris, P.D.; van Osch, D.J.G.P.; Cremers, G.J.W.; Boot, M.D.; Hensen, E.J.M. Mild thermolytic solvolysis of technical lignins in polar organic solvents to a crude lignin oil. *Sustain. Energy Fuels* **2020**, *4*, 6212–6226. [CrossRef]

52. Huang, X.; Korányi, T.I.; Boot, M.D.; Hensen, E.J.M. Catalytic Depolymerization of Lignin in Supercritical Ethanol. *ChemSusChem* **2014**, *7*, 2276–2288. [CrossRef]

53. Kim, Y.; Shim, J.; Choi, J.-W.; Jin Suh, D.; Park, Y.-K.; Lee, U.; Choi, J.; Ha, J.-M. Continuous-flow production of petroleum-replacing fuels from highly viscous Kraft lignin pyrolysis oil using its hydrocracked oil as a solvent. *Energy Convers. Manag.* **2020**, *213*, 112728. [CrossRef]

54. Zhang, L.; Luo, Y.; Wijayapala, R.; Walters, K.B. Alcohol Stabilization of Low Water Content Pyrolysis Oil during High Temperature Treatment. *Energy Fuels* **2017**, *31*, 13666–13674. [CrossRef]

55. de Waard, D.F.; Kouris, P.D.; Boot, M.D.; Hensen, E.J.M. Mixed Cu–Mn Oxide Catalysts for Solvolysis of Technical Lignin. *ACS Sustain. Chem. Eng.* **2025**, *13*, 3269–3279. [CrossRef] [PubMed]